Vortex Flow Over Delta and Double-Delta Wings

H.W.M. Hoeijmakers* and W. Vaatstra†
National Aerospace Laboratory NLR, Amsterdam, the Netherlands
and
N.G. Verhaagen‡
Delft University of Technology, Delft, the Netherlands

A theoretical and experimental investigation of the flow about a slender delta wing and two double-delta wings is described. The objective of the investigation is to develop accurate computational methods for the vortex flow about slender wings and strake-wing configurations. Numerical results of computational methods developed for the flow about slender wings are compared with experimental results of the present and also of earlier investigations. It is demonstrated that satisfactory numerical results are obtained for the normal force, pressure distribution, as well as vortex position and vortex sheet geometry. It is shown that for analyzing the structure of complex vortex flow the laserlight-sheet flow visualization technique is very useful. Results of the flow visualization are presented for the flow about the delta wing and the double-delta wing. Based on the results for the double-delta wings, a new vortex sheet model is proposed for these wings involving a single-branched strake vortex and a double-branched wing vortex.

Nomenclature

$\mathcal{R}$ = aspect ratio = b^2/S_{ref}
a = cot Λ
b = span
C_N = normal force coefficient = (normal force)/$q_\infty S_{ref}$
C_p = pressure coefficient = $(p-p_\infty)/q_\infty$
c = root chord
e_x = unit vector in x direction
LDV = laser Doppler velocimeter
L.E. = leading edge
n = normal vector
p = pressure
p_∞ = freestream pressure
q_∞ = dynamic pressure = $\frac{1}{2}\rho U_\infty^2$
s_f = farwake cutoff length
S_p = feeding sheet
S_{ref} = wing reference area
S_v = vortex sheet
S_w = wing surface
s,t = surface coordinates
s^*,t^* = panel midpoint
T = leading-edge vortex sheet cutoff length
T.E. = trailing edge
U_∞ = freestream velocity
u = velocity vector
$X(t)$ = (position vector in cross-flow plane)/(local span)
X_v = (position of vortex)/(local span)
x = (Cartesian coordinate, directed along wing centerline)/c
$\bar{x}$ = (coordinate in freestream direction)/c
$x(s,t)$ = (position vector of surface)/c
$x_v(s)$ = (position vector of vortex)/c
x = vector cross product
= vector dot product
y = (Cartesian coordinate, directed in starboard direction)/c
z = (Cartesian coordinate, perpendicular to x and y)/c
α = angle of attack, deg
α_0 = angle of attack at zero lift
γ = vorticity vector
Δ = jump in quantity across surface
Λ = sweep angle, deg
$\mu(s,t)$ = surface doublet distribution
ρ = fluid density
$\rho(t)$ = contour doublet distribution
τ = timelike coordinate = $(x-1)\tan\alpha/\cot\Lambda$
ϕ = velocity potential

Presented as Paper 82-0949 at the AIAA/ASME Third Joint Thermophysics, Fluids, Plasma and Heat Transfer Conference, St. Louis, Mo., June 7-11, 1982; submitted July 7, 1982; revision received Feb. 25, 1983.

*Research Engineer, Fluid Dynamics Division. Member AIAA.
†Research Engineer, Informatics Division.
‡Research Associate, Department of Aerospace Engineering.

Introduction

SEPARATION induced vortex flow from leading and side edges is of increasing importance for the high-angle-of-attack aerodynamics of various modern aircraft. Examples are aircraft designed for high speed, employing slender wing concepts with highly swept and relatively sharp leading edges, and aircraft designed for maneuvering, often employing the strake-wing concept. Until now, the design of wings employing vortex lift has been almost entirely empirical, the resulting wing shape being the result of laborious cut-and-try-type wind tunnel programs.

However, if the vortex-lift capabilities of slender wings or strake-wing configurations are to be fully understood and utilized, computational methods for the determination of the detailed structure of the flowfield are required. The possibilities of computing vortex flow characteristics for such configurations are, at present, rather limited. The most widely used method is to employ the Polhamus suction analogy.[1] This empirical method provides the forces and moments on the configuration, and can be applied in subsonic and in supersonic flow, but does not predict the pressure and velocity distributions. For the flow about slender wings, Refs. 2-5 describe the development of methods capable of computing the detailed velocity and pressure distributions. In the vortex-lattice-type approach, used in Refs. 2 and 3, the vortex sheet is modeled by discrete line vortices. In this approach, the identity of the vortex sheet is lost and the method is inadequate for highly rolled-up vortex sheets. In the second-order panel method employed in Refs. 4 and 5, the vortex sheet is more accurately modeled, but it has proven to be difficult to define a numerically stable computational scheme. A drawback of using the panel method is that, a priori, the

global structure of the vortex sheets is required. In addition, only linear compressible flows can be dealt with. The current free-vortex-sheet methods are restricted to configurations with a vortex sheet rolling up into one concentrated vortex core. The core is modeled using a relatively simple isolated vortex model. A more accurate modeling of the vortex cores in the free-vortex-sheet model is one of the key problems in modeling vortex flow. Recently Eriksson and Rizzi[6] have solved Euler's equations for the transonic and supersonic flow about a slender delta wing. Employing a dissipative numerical scheme, the vortex sheet and cores are "captured" instead of "fitted," quite similar to the capturing of shock waves in current transonic flow computations. A major advantage of this "artificial viscosity" method is that it requires no a priori knowledge about the topology of the vortex flow.

For the vortex flow about strake-wing configurations, a clearly defined computational model is not available at present. Investigations by Luckring,[7] Lamar,[8] and, in particular, Brennenstuhl and Hummel[9] have been valuable in gaining insight into the complicated topology of the vortex layer structure above a strake-wing configuration. However, certain fundamental points still need clarification. In particular, details of the shape of the strake leading-edge vortex layer downstream of the kink are unclear.

In an attempt to shed further light on some of the above mentioned points, NLR and the Delft University of Technology are conducting a collaborative research program. The objective of the program is to obtain a reliable and physically relevant computational method for determining the detailed aerodynamic characteristics of configurations with vortex flow. The research program contains the following elements:

1) Visualization of the flow pattern by means of a laserlight-sheet technique.

2) Detailed flowfield measurements with a total pressure probe, a five-hole probe, and LDV equipment to determine the characteristics of vortex cores (i.e., entrainment[10]).

3) Development of computational methods and comparison with experimental results.

Although it is recognized that vortex flow is of importance at high subsonic and transonic speeds, in the present investigation only the case of vortex flow at low speeds is considered.

The purpose of this paper is to provide an overview of the research on delta wing and double-delta wing vortex flow conducted so far at NLR and the Department of Aerospace Engineering at the Delft University of Technology. After briefly describing the main features of the physics of leading-edge vortex flow, the experimental setup is described, followed by a description of the computational methods developed. Finally, results of the present theoretical and experimental investigation will be presented.

Physics of Leading-Edge Vortex Flow

The topology of the high-Reynolds-number flow about slender wings with leading-edge vortex separation has been well established in experimental investigations by, amongst others, Earnshaw[11] and Hummel.[12]

At moderate to high angles of attack, the flow separates at the highly swept leading edge, with the boundary layers flowing off the upper and lower surface merging into a free shear layer. Under the influence of the vorticity contained in it, the shear layer rolls up in a spiral fashion to form concentrated cores with distributed vorticity. The presence of such cores in the proximity of the wing surface affects the pressure distribution to a large extent. On slender planforms, large vortex-lift increments are produced, and a stable flow pattern has been observed up to 30 or 35 deg. A limit to the favorable effects induced by the vortex flow is reached when the angle of attack has reached a value at which large-scale vortex breakdown occurs above the wing.

Experimental Setup

Wind Tunnel and Test Conditions

The experimental part of the investigation has been carried out in the low-speed wind tunnel of the Department of Aerospace Engineering at the Delft University of Technology. The wind tunnel has an octagonal test section, 1.25 m high by 1.80 m wide and a turbulence level of about 0.05% at the speed of 30 m/s used in the present investigation. The Reynolds number based on the root chord of the models was 1.4×10^6.

Models

The planform of the three models is shown in Fig. 1. Model I is a sharp-edged 76-deg swept delta wing ($AR = 1$). The vortex flow for such a slender delta wing is well organized, stable, and symmetric up to 35 deg, and therefore well suited for studying vortex flow. Models II and III are sharp-edged double-deltas, i.e., simplified strake-wing configurations. For both models, the strake, i.e., the forward half of the planform, has a leading-edge sweep of 76 deg. The wing, i.e., the rearward half of models II and III, has a sweep of 60 and 40 deg, respectively. Model II is representative for the planform of high-speed aircraft, while model III is representative for the planform of several contemporary highly maneuverable aircraft. In the model definition phase it was theorized that model II would exhibit a vortex system with the leading-edge shear layer attached all along the leading edge exhibiting one or two vortex cores. For model III, with its reduced leading-edge sweep, it was expected that, at least at low α, the flow on the outboard part of the wing would be attached. Thus the leading-edge shear layer would emanate from the strake leading edge only. At higher α, the flow about models II and III would have the same appearance. It should be emphasized that in case of rounded wing leading edges the flow on the outboard part of the wing may be attached up to a higher α than observed in the present investigation. The three models are flatplate-type Duraluminum models with sharp leading and trailing edges. The models have a root chord c of 0.667 m, a maximum thickness/chord ratio of 0.03, and a leading-edge thickness of 0.2 mm. These edges were chamfered on the windward side of the model only. This left the leeward side flat, simplifying the flowfield investigation.

Laserlight Sheet

To visualize the rolling-up shear layers and the vortex cores, smoke (heated paraffin oil droplets) was injected into the flow at a position upstream of the apex of the model. The smoke was illuminated by a thin sheet of intense light perpendicular to the freestream direction. This sheet was produced by a 5-W argon-ion laser in conjunction with an optical system. The laser was mounted on a traversing platform, enabling a translation in the freestream direction, thereby visualizing the streamwise development of the vortex flow. A schematic view of the setup is shown in Fig. 2. The flow pattern was photographed by a remotely controlled camera positioned downstream of the model. In addition, the flow pattern was recorded on video tape.

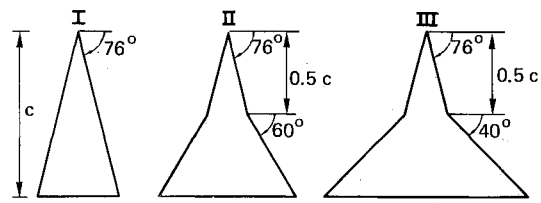

Fig. 1 Wind tunnel models.

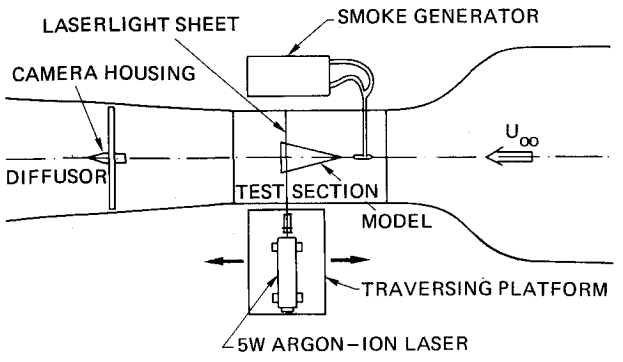

Fig. 2 Schematic of laserlight-sheet setup.

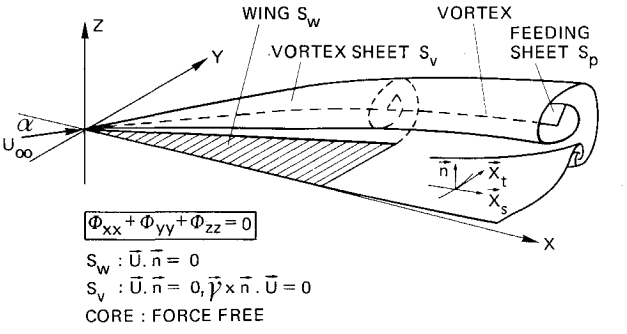

Fig. 3 Mathematical model of flow over a slender wing.

Computational Methods

This section describes computational methods developed for computing the vortex flow about slender delta-like wings. A computational method for the vortex flow about double-delta wings and strake-wing configurations, based on the model derived in the present laserlight-sheet investigation, is presently being pursued and will be reported on in the near future. First, the mathematical model is described, followed by the description of the computational methods.

Mathematical Model

The mathematical model of high-Reynolds-number leading-edge vortex flow is based on earlier studies (see Refs. 13-15). This free-vortex-sheet model, depicted in Fig. 3 for the case of a slender delta wing, has been used in Refs. 2-5. In this inviscid model, the shear layers emanating from the leading and trailing edges are represented by vortex sheets embedded in an otherwise irrotational flow. The leading-edge vortex core, which in inviscid flow is a tightly wound spiraling vortex sheet of infinite extent, is modeled by a isolated line vortex connected to the remainder of the sheet by a so-called feeding sheet. To model the entrainment of the rotational core, it has been proposed to assign a sink strength to the line vortex as well.[5] The model described is based on neglecting 1) the occurrence of boundary-layer separation, resulting in secondary, tertiary, etc., vortex systems; 2) flow conditions at which the vortex system turns asymmetric; and 3) vortex breakdown above the wing. Assuming incompressible flow, the problem is governed by Laplace's equation for the velocity potential $\phi(x,y,z)$:

$$\phi_{xx}+\phi_{yy}+\phi_{zz}=0 \tag{1}$$

where the velocity is given by $\boldsymbol{u}=\nabla\phi$.

For subsonic compressible flow, it is expected that the Göthert transformation, which replaces Eq. (1) by the Prandtl-Glauert equation, will yield reliable results.[16] The boundary conditions that apply on the wing and vortex sheet are (see Fig. 3):

1) Zero normal velocity, both on the wing S_w as on the vortex sheet S_v, i.e.,

$$\boldsymbol{u}\cdot\boldsymbol{n}=0 \tag{2}$$

2) Zero pressure jump across the vortex sheet S_v, i.e.,

$$\Delta C_p=C_p^+-C_p^-=0 \tag{3a}$$

With Bernoulli's equation and Eq. (2), Eq. (3a) can be expressed as

$$\boldsymbol{\gamma}\times\boldsymbol{n}\cdot\boldsymbol{u}=0 \tag{3b}$$

where $\boldsymbol{\gamma}$ is the vorticity vector.

3) The model of the core is force free; i.e., the component normal to the vortex of the sum of the force on the vortex and the force on the feeding sheet is zero. This condition is the three-dimensional analog of the conical flow formulation of Smith.[15]

The potential flow problem is solved by employing a surface doublet distribution to model both the wing surface and the vortex sheets. By imposing the boundary conditions 1-3, a solution is sought for the unknown doublet distribution on the wing and the vortex sheet, for the unknown geometry of the vortex sheet, and for the unknown position of the vortex core. Because of the nonlinearity associated with the unknown position of vortex sheet and vortex core, an iterative solution procedure must be employed.

The solution of the problem is conveniently described in a computational plane on which a surface coordinate system is defined. In this formulation, S_w and S_v are given as $x=x(s,t)$, where s is approximately in streamwise direction and t is in the cross-flow plane. In the computational plane, the surface comprising both the wing and the vortex sheet becomes a rectangular domain (see Fig. 4). The doublet distribution on this domain is denoted as $\mu(s,t)$. More details of the present formulation are found in Ref. 5. Because of the complexity of the fully three-dimensional problem, it has been found useful to consider two quasi-two-dimensional limiting cases, namely, the case of conical flow and the case of two-dimensional time-dependent vortex wake roll-up (see Fig. 4). The primary objective of considering these two cases has been to study various possible numerical schemes for the fully three-dimensional problem. Additional benefits are: 1) the influence of the choice of parameters such as sheet length can be studied at less expense and in greater detail; 2) with the solutions of the quasi-two-dimensional problems, a reasonable initial guess for the solution of the fully three-dimensional problem can be constructed; and 3) a first insight is obtained in the influence of changing the cross-sectional geometry (e.g., leading-edge camber, vortex flaps).

Conical Flow Method—VORCON

Observation of the flow over the forward two-thirds of slender delta wings suggests that even at subsonic speeds the flow is nearly conical, except possibly in the region very near the apex. The assumption of conical flow is only valid for wings with straight, highly-swept leading edges, for which the slender-body theory also applies. Conical flow implies that on S_v and S_w

$$x(s,t)=se_x+asX(t) \tag{4a}$$

$$\mu(s,t)=as\rho(t) \tag{4b}$$

where $X(t)$ is a vector in the cross-flow plane. The position of the vortex core is written as

$$x_v(s)=se_x+asX_v \tag{4c}$$

where X_v is the vortex position in the cross-flow plane.

Substitution of Eqs. (4a), (4b), and (4c) into the boundary conditions and expansion for the small value of a results in a

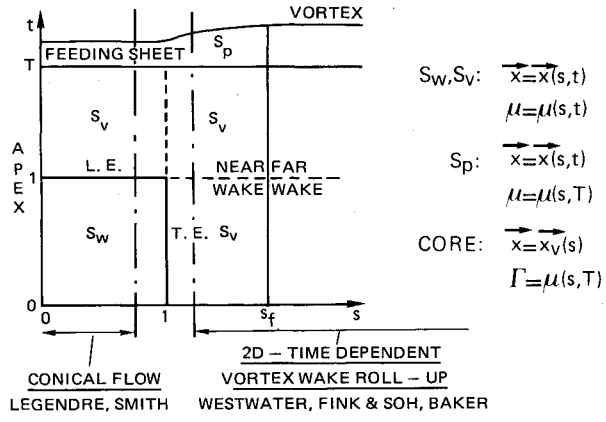

Fig. 4 Computational domain.

two-dimensional problem in the cross-flow plane. Legendre,[13] Brown and Michael,[14] Smith,[15] and others have solved the conical flow problem by means of conformal mapping the wing onto the symmetry plane, thereby automatically satisfying Eq. (2) on S_w. The resulting problem is to solve for the shape and strength of the vortex sheet and position of the vortex in the transformed plane. This is accomplished using a panel-method-type approach in this plane. In the present method, described in more detail in Ref. 17, a panel method is applied in the physical plane instead, so that no conformal mapping is needed and an arbitrary cross section can be analyzed quite easily.

The wing and vortex sheet are divided into segments (panels), and the doublet distribution $\rho(t)$ and the geometry $X(t)$ are approximated by panelwise quadratic representations, e.g.,

$$\rho(t)=\rho^*+(t-t^*)\rho_t^*+\tfrac{1}{2}(t-t^*)^2\rho_{tt}^* \tag{5}$$

where t^* denotes the panel midpoint, and ρ^*, ρ_t^*, and ρ_{tt}^* denote the function value and the first and second derivatives of $\rho(t)$ with respect to t at $t=t^*$, respectively. The derivatives in Eq. (5) are approximated by second-order accurate finite difference expressions. This results in a quadratic representation that, in general, is discontinuous in function value and its derivatives across panel edges. Since these discontinuities are small, at higher order they are neglected. This also avoids spurious effects due to discrete vortices of strength equal to the jump in the doublet distribution across the panel edges.[4] Finding a stable numerical scheme for the mixed analysis/design-type boundary conditions has proven to be difficult. In the computer code developed for the limiting case of conical flow, designated VORCON, numerical stability is provided by a four-point difference scheme. This scheme, described in Ref. 17, involves function values at panel edges in combination with collocation at panel midpoints. However, the extension of this scheme to the three-dimensional case has proved to result in numerical instabilities. An alternative to the scheme presented in Ref. 17 is to use function values at midpoints and to employ a backward difference scheme for the first derivative, a central difference scheme for the second derivative in combination with collocation at the midpoints. It is the bivariate counterpart of this scheme that is currently being employed for the fully three-dimensional problem.

Two-Dimensional Time-Dependent Vortex Wake Roll-Up Method—VOR2DT

The second limiting case concerns the problem of vortex wake roll-up downstream of the delta wing. Assuming that the derivatives in the x direction are small compared with those in the cross-flow plane, the original three-dimensional steady problem is reduced to a two-dimensional time-dependent problem by replacing x by $U_\infty\tau$, where τ is a timelike variable. The resulting problem is an initial value problem describing the motion of a two-dimensional vortex sheet as it is convected with the local flow velocity in subsequent cross-flow planes. The initial conditions of the problem are the shape of the trailing (shedding) edge of the wing and the distribution of the shed vorticity (or load) distribution. Using a discrete vortex approximation, this model has been used by Westwater,[18] Moore,[19] Maskew,[20] and many others to compute the evolution of the wake behind a trailing edge.

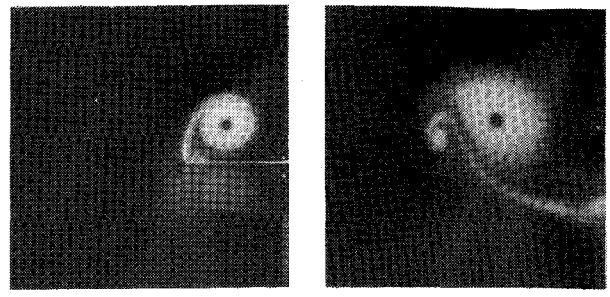

Fig. 5 Vortex flow about model I, $\alpha=20$ deg.

However, it appears that this type of approximation results in numerical instabilities when the number of discrete vortices is increased. The technique of periodic rediscretization, as introduced by Fink and Soh,[21] for suppressing these instabilities succeeded in solving this problem. However, recent investigations by Baker[22] for a case where a double-branched spiral evolves have shown that this method eventually ends in chaos as well. By using the panel method described for the conical flow problem and by modeling highly rolled-up regions, i.e., single-branched and double-branched vortices by vortex-feeding-sheet(s) combinations, a reliable computational procedure is obtained. This procedure, designated VOR2DT, is described in more detail in Ref. 23, where it is also demonstrated that the wake behind a delta wing can be computed quite realistically.

Three-Dimensional Vortex Flow Method—VORSEP

For solving the fully three-dimensional problem, the computational domain, depicted in Fig. 4, is divided into rectangular panels. Panelwise representations for the unknown bivariate functions $\mu(s,t)$ and $x(s,t)$ are obtained from products of spline-type representations in one variable, e.g.,

$$\mu(s,t)=\mu^*+(s-s^*)\mu_s^*+(t-t^*)\mu_t^*+\tfrac{1}{2}(s-s^*)^2\mu_{ss}^*$$
$$+(s-s^*)(t-t^*)\mu_{st}^*+\tfrac{1}{2}(t-t^*)^2\mu_{tt}^* \tag{6}$$

where (s^*,t^*) denotes the panel midpoint, and μ^*, μ_s^*, μ_t^*, etc., denote the value of μ, μ_s, μ_t, etc., at this point. The derivatives in Eq. (6) are approximated by second-order accurate finite-difference expressions, involving function values at midpoints. For second derivatives, a central difference scheme is used. For first derivatives, a backwards difference scheme is used. The midpoints are taken as the collocation points. Details of the iterative procedure for solving the resulting set of nonlinear equations are provided in Ref. 5.

Results for Delta Wing

This section presents the results of the flow visualization investigation employing the laserlight-sheet technique and compares the results of the VOR codes with experimental results for model I and other delta wings.

Flow Visualization

The flow pattern is illustrated quite clearly by the laserlight-sheet pictures presented in Fig. 5, which shows the flow about

model I at $\alpha = 20$ deg. Shown are the patterns at 75% and at 150% root chord. The spiraling shear layer emanating from the leading edge increases in thickness with increasing distance from the leading edge. When its thickness is such that consecutive turns of the spiraling layer overlap, viscous diffusion results in a region of continuously distributed vorticity (the leading-edge vortex core). Inside this rotational core, the circumferential velocity is so high,[11] that no smoke particles can enter the region. It shows up as the black spot in Fig. 5. Inside the leading-edge vortex core there is a strong interaction between the swirl and axial velocity. The latter may reach values several times that of the freestream velocity.[11] In the wake of the wing, the vorticity of sign opposite to the vorticity in the leading-edge shear layer rolls up into a double-branched core, the so-called trailing-edge vortex. This phenomenon has been studied experimentally by Hummel[12] and earlier by Maltby.[24]

Numerical Results and Comparison with Experiments

In Fig. 6, the position of the leading-edge vortex and trailing-edge vortex computed for the case without thickness by VORCON/VOR2DT and VORSEP are compared with experimental data for model I at $\alpha = 20$ deg. The correlation of the results of the two quasi-two-dimensional codes with experimental data is excellent, except near the trailing edge, where the assumptions underlying both models are violated. The code for the three-dimensional flow, VORSEP, does not account for the trailing-edge vortex, resulting partly in the deviations apparent in Fig. 6.

Model I does not provide the pressure distribution, so computed pressures are compared here with the experimental results of Hummel and Redeker[25] and of an earlier investigation at Delft University[26] for the same planform but with different cross sections.

Figure 7 compares the pressure distributions, as computed by VORCON and VORSEP, with the measured distributions. In the experiment of Ref. 25, the boundary layer was turbulent, while in the experiment of Ref. 26 the boundary-layer transition took place at approximately 60% root chord. Outboard of the suction peak, secondary separation effects are evident in both experiments. Up to 50% root chord, the conical flow solution agrees quite satisfactorily with experimental data. On this part of the wing the three-dimensional solution slightly overpredicts the suction peak underneath the vortex core. As is evident from Fig. 7, the conical flow solution does not apply near the trailing edge. In general, the VORSEP solution shows satisfactory correlation with experimental data. Figure 8 compares the computed normal force with experimental data obtained in the present investigation and the data obtained by Verhaagen.[26]

Since in the conical flow method the trailing-edge Kutta condition is not accounted for, VORCON overpredicts the normal force. The normal force predicted by the VORSEP program is in much better agreement with experiment. Figure 9 shows the shape of the vortex sheet at various streamwise stations as computed by VORSEP. In the wake, the sheet extends over a length of only 1.9 times the half span of the wing, which in this case means that at $x = 1.5$ the trailing vortex is combined with the leading-edge vortex and does not show up. Subsequent computations have shown that increasing the length of the sheet in the cross-flow plane and increasing the panel density result in more realistic sheet shapes. Also note that sheet shapes computed with the VOR2DT code for a much finer panel scheme than would be feasible for VORSEP, reported in Ref. 23, clearly show the same features as observed in experiment.

Figure 10 compares the computed conical and three-dimensional sheet shapes at $\alpha = 20$ deg for two streamwise stations. Both Figs. 9 and 10 indicate that the solution of the fully three-dimensional problem, as far as the shape of the sheet and the position of the vortex are concerned, is conical almost up to the trailing edge. However, the doublet distribution computed by VORSEP deviates already from the conical value computed by VORCON on the forward part of the delta wing. This is clearly shown in the right part of Fig. 10 and is also evident from the computed pressures shown in Fig. 7.

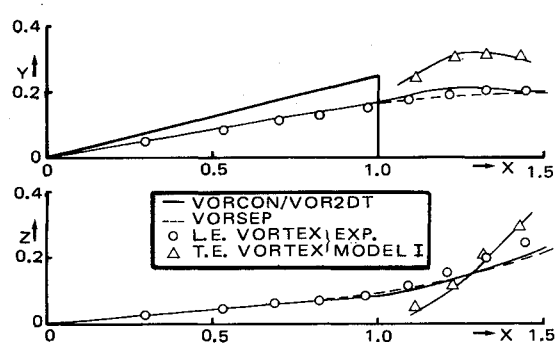

Fig. 6 Position of delta wing vortex cores, $\alpha = 20$ deg.

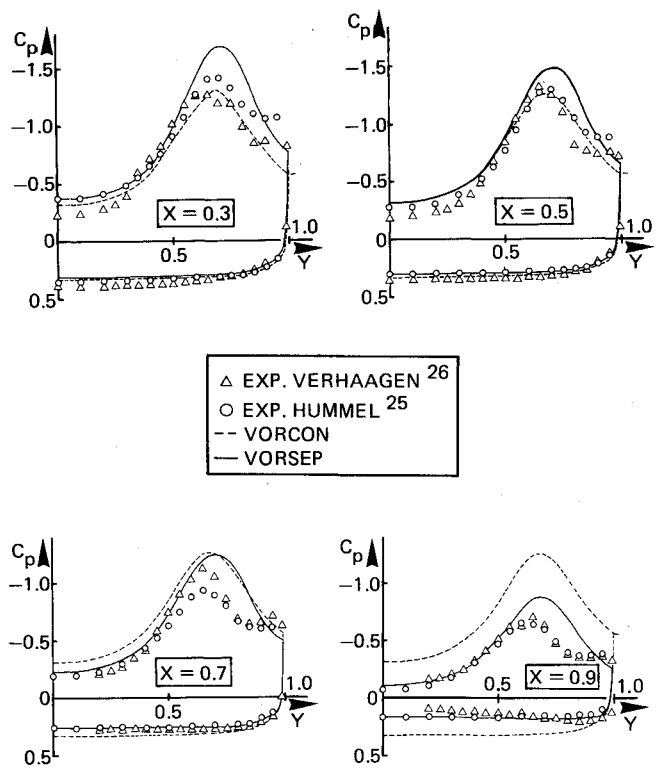

Fig. 7 Computed and measured pressure distributions, $\alpha = 20$ deg.

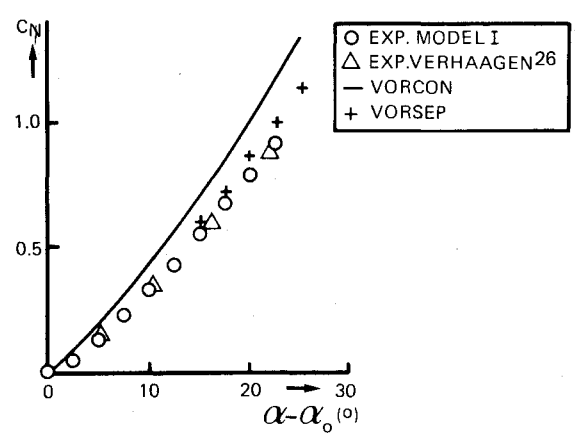

Fig. 8 Computed and measured normal forces.

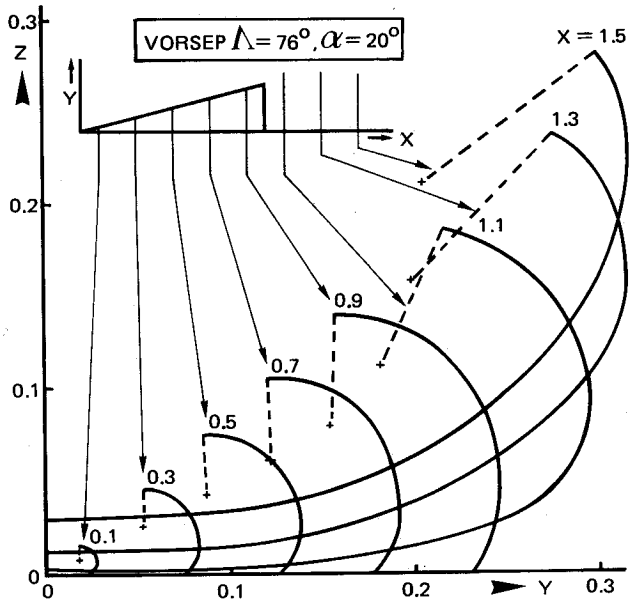

Fig. 9 Vortex-sheet shapes computed with VORSEP.

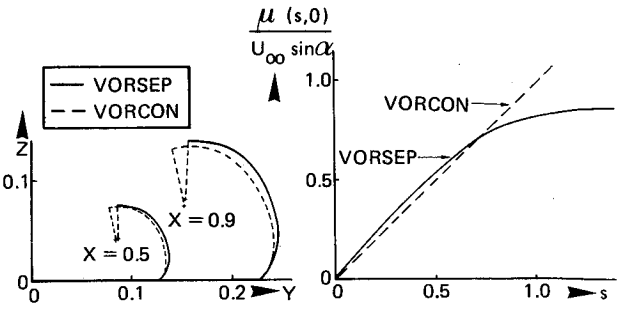

Fig. 10 Comparison of VORCON and VORSEP solution.

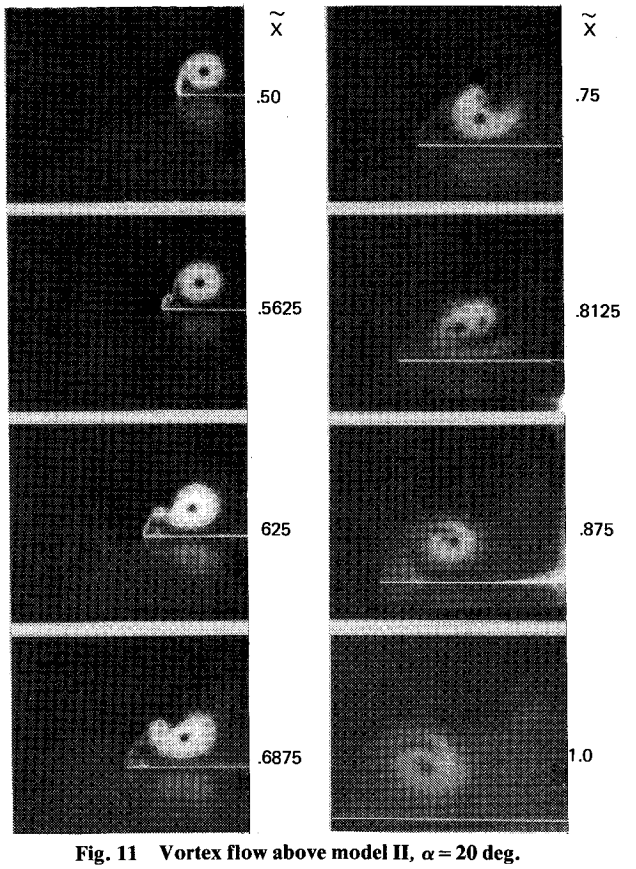

Fig. 11 Vortex flow above model II, $\alpha = 20$ deg.

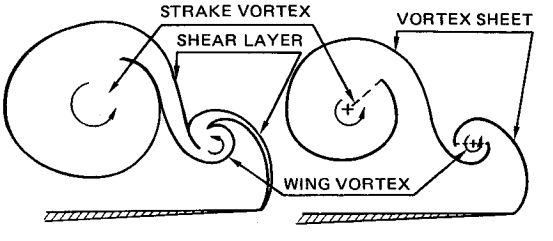

Fig. 12 Schematic of double-delta vortex flow.

Results for Double-Delta Wings

This section presents results of the investigation into the structure of the flow employing the laserlight-sheet technique. The investigation will be described in greater detail in Ref. 27.

Double-Delta Model II

Figure 11 shows the results of the flow visualization for $\alpha = 20$ deg. Above the forward half of the wing, the shear layer emanating from the leading edge rolls up into the (single-branched) strake vortex. Downstream of the kink, the shear layer remains attached to the leading edge. In this layer a double-branched vortex core, generally called the wing vortex, develops (see left half of Fig. 12). One branch of the vortex is connected to the leading edge, while the second branch is connected to the strake vortex. Presumably all the vorticity in the layer is of the same sign, suggesting that the wing vortex increases in strength because it is fed with vorticity from the wing leading edge as well as from the shear layer emanating from the strake leading edge. In the downstream direction, the wing vortex, embedded in the shear layer, travels along this layer, thereby looping around the strake vortex. The wing vortex remains distinguishable in Fig. 11 up to the trailing edge. However, because of the viscous diffusion, the rolling-up shear layer, with the wing vortex embedded, forms a region of continuously distributed vorticity. This region encompasses the inner loops of the shear layer and both the wing vortex core and the strake vortex core. Downstream of the trailing edge, the two vortex cores have essentially merged. Thus, here the flow pattern resembles the one behind a conventional delta wing (Fig. 5).

The position of the strake and wing vortex has been determined from the laserlight-sheet photographs. Figure 13 shows the lateral position of both strake and wing vortex together with the schematic cross-sectional structure of the vortex flow as conjectured from Fig. 11. Although this figure presents the vortex flow topology for $\alpha = 20$ deg, it is found to be representative for angles of attack between 10 and 25 deg. Further experimental investigation of the detailed pressure and velocity distribution above the wing will be needed to support or correct the above conjectured flow topology. For model II, vortex breakdown was observed at $\alpha = 25$ deg, namely, downstream of the trailing edge at $\tilde{x} = 1.5$. For a delta wing with 60-deg leading-edge sweep, vortex breakdown has been observed at the trailing edge for angles of attack as low as 13 deg.[28] This demonstrates that the vortex flowfield has been stabilized considerably by adding the strake.

Double-Delta Model III

The laserlight-sheet visualization of the vortex flow above model III at $\alpha = 20$ deg shows a similar flow pattern as that observed for model II. The main difference is that, in this case, vortex breakdown occurs above the wing before the strake vortex and wing vortex have coalesced into one region of distributed vorticity. Primarily because of the reduced leading-edge sweep, the wing vortex is weaker than for model II, which results in a weaker interaction of strake and wing vortex. However, the wing vortex is again a double-branched vortex embedded in the shear layer from the wing leading

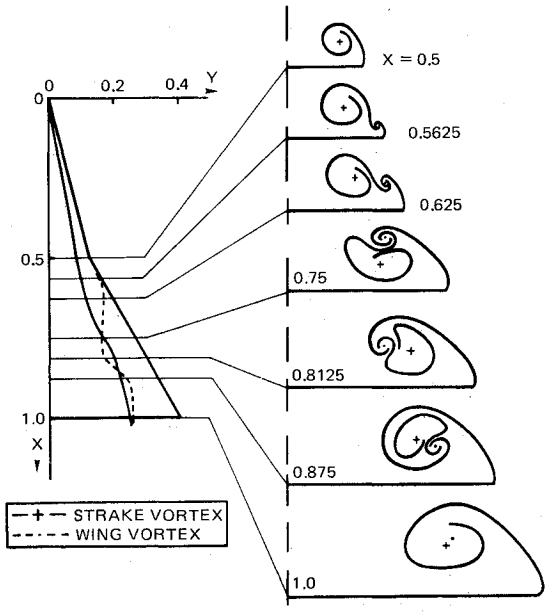

Fig. 13 Conjectured flow pattern model II, $\alpha = 20$ deg.

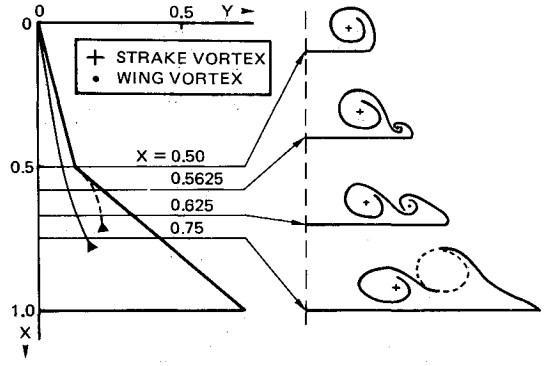

Fig. 14 Conjectured flow pattern model III, $\alpha = 20$ deg.

edge. The conjectured flow pattern is depicted in Fig. 14. In the present investigation, the strake leading-edge vortex layer did not detach from the wing leading-edge vortex layer. However, at α below 10 deg, where the wing leading-edge vortex layer becomes weak, and close to the wing upper surface, the situation is not completely clear. Reducing the wing leading-edge sweep or rounding the wing leading edge may result, at least for low α, in a flow pattern with only a shear layer emanating from the strake leading edge.

Double-Delta Vortex Sheet Model

In order to enable a VORSEP-like potential flow computation for the flow about double-delta configurations, a vortex sheet model is required. Based on the present interpretation, the vortex sheet model depicted in the right half of Fig. 12 is proposed. All along the leading edge of the double-delta wing the vortex sheet is attached to the edge. Above the strake, this vortex sheet ends in a vortex-feeding sheet combination which models the strake vortex. Downstream of the kink, the wing vortex is modeled by a vortex connected to the remainder of the sheet by feeding sheets, similar to the model used in VOR2DT.[23] This model will be used to extend the capability of VORSEP to double-delta configurations. The present interpretation of the vortex flowfield resolves the problem with the schematic models proposed in Refs. 7-9, where the strake vortex sheet tears apart at the kink, leaving an unrolled "loose end" of a vortex sheet in the flowfield. It is suggested in Ref. 29 that this end rolls up into a vortex core with circulation of sign opposite to the sign of the circulation of the strake vortex. Seen in the light of the present investigation, this seems incorrect.

Concluding Remarks

Insight into the vortex flow about delta and double-delta wings is obtained employing the very useful laserlight-sheet technique. The present investigation indicates that the flow pattern above sharp-edged double-delta wings consists of a single-branched strake vortex and a double-branched wing vortex. The latter originates at the kink and is embedded in the shear layer from the leading edge. Based on this interpretation, a vortex-sheet model is postulated. Numerical results are presented for the flow about a 76-deg swept delta wing, obtained with a free-vortex-sheet method for the fully three-dimensional problem, one for the limiting case of conical flow and one for the limiting case of vortex wake roll-up. It has been demonstrated that satisfactory numerical results can be obtained for delta wings. It is expected that with the gained insight into the double-delta wing vortex flow pattern the present free-vortex-sheet method can be extended to the case of strake-wing configurations.

To support further theoretical investigations into vortex flow, detailed measurements of pressure and velocity distributions will be needed, the latter especially with the objective of obtaining the characteristics of vortex cores and defining an appropriate computational model for these cores.

Acknowledgments

A portion of the theoretical investigation described in this paper was carried out under contract for the Scientific Research Division of the Directorate of Materiel of the Royal Netherlands Air Force, RNLAF. The authors gratefully acknowledge the Audio-Visual Center of the Delft University of Technology for their assistance in filming the laserlight-sheet investigation as well as the VOR2DT results.

References

[1] Polhamus, E.C., "Prediction of Vortex-Lift Characteristics by a Leading-Edge Suction Analogy," *Journal of Aircraft*, Vol. 8, April 1971, pp. 193-199.

[2] Rehbach, C., "Numerical Calculation of Three-Dimensional Unsteady Flows with Vortex Sheets," AIAA Paper 78-111, Jan. 1978.

[3] Kandil, O.A. and Balakrishan, L., "Recent Improvements in the Prediction of Leading and Trailing Edge Vortex Cores of Delta Wings," AIAA Paper 81-1263, June 1981.

[4] Johnson, F.T., Tinoco, E.N., Lu, P., and Epton, M.A., "Three-Dimensional Flow over Wings with Leading-Edge Vortex Separation," *AIAA Journal*, Vol. 15, April 1980, pp. 367-380.

[5] Hoeijmakers, H.W.M. and Bennekers, B., "A Computational Method for the Calculation of the Flow about Wings with Leading-Edge Vortices," AGARD CP-247, 1979.

[6] Eriksson, L.-E. and Rizzi, A., "Computation of Vortex Flows around Wings Using the Euler Equations," *Proceedings of the 4th GAMM-Conference on Numerical Methods in Fluid Mechanics*, edited by H. Viviand, Vieweg Verlag, Paris, 1981, pp. 87-105.

[7] Luckring, J.M., "Aerodynamics of Strake-Wing Configurations," *Journal of Aircraft*, Vol. 16, Nov. 1979, pp. 756-762.

[8] Lamar, J.E., "Analysis and Design of Strake-Wing Configurations," *Journal of Aircraft*, Vol. 17, Jan. 1980, pp. 20-27.

[9] Brennenstuhl, U. and Hummel, D., "Untersuchungen über die Wirbelbildung an Flügeln mit geknickten Vorderkanten," *Zeitschrift für Flugwissenschaften und Weltraumforschung*, Vol. 5, 1981, pp. 375-381; see also DGLR-Vortrag 81-046 and 81-256.

[10] Verhaagen, N.G. and Snoek, L.v.d., "An Experimental Investigation of the Entrainment into a Leading-Edge Vortex," Dept. of Aeronautical Engineering, Delft University of Technology, Delft, the Netherlands, Report LR-322, 1981; see also AGARD CP-247, 1979.

[11] Earnshaw, P.B., "An Experimental Investigation of the Structure of a Leading-Edge Vortex," Aeronautical Research Council, R&M No. 3281, 1962.

[12] Hummel, D., "On the Vortex Formation Over a Slender Wing at Large Incidence," AGARD-CP-247, 1979.

[13]Legendre, R., " Ecoulement au Voisinage de la Pointe avant d'une Aile à Fortè Fleche aux Incidences Moyennes," *La Recherche Aérospatiale*, Vol. 30, Nov. 1952, pp. 3-8; Vol. 31, Jan. 1953, pp. 3-6; and Vol. 35, Sept. 1953, pp. 7-8.

[14]Brown, C.E. and Michael, W.H., "Effect of Leading-Edge Separation on the Lift of a Delta Wing," *Journal of Aeronautical Sciences*, Vol. 21, Oct. 1954, pp. 690-694.

[15]Smith, J.H.B., "Improved Calculations of Leading-Edge Separation from Slender, Thin, Delta Wings," *Proceedings of the Royal Society of London, Series A*, Vol. 306, 1968, pp. 69-90.

[16]Luckring, J.M., Schoonover, W.E., and Frink, N.T., "Recent Advances in Applying Free Vortex Sheet Theory for the Estimation of Vortex Flow Aerodynamics," AIAA Paper 82-0095, 1982.

[17]Hoeijmakers, H.W.M. and Vaatstra, W., "A Higher-Order Panel Method for the Computation of the Flow about Slender Delta Wings with Leading-Edge Vortex Separation," *Proceedings of the 4th GAMM-Conference on Numerical Methods in Fluid Mechanics*, edited by H. Viviand, Vieweg Verlag, Paris, 1981, pp. 137-149; see also National Aerospace Laboratory, Amsterdam, the Netherlands, NLR MP 81053 U, 1981.

[18]Westwater, F.L., "Rolling Up of the Surface of Discontinuity Behind an Aerofoil of Finite Span," Aeronautical Research Council, R&M No. 1962, 1935.

[19]Moore, D.W., "A Numerical Study of the Roll-Up of a Finite Vortex Sheet," *Journal of Fluid Mechanics*, Vol. 63, Pt. 2, 1974, pp. 225-235.

[20]Maskew, B., "Subvortex Technique for the Close Approach to a Discretized Vortex Sheet," *Journal of Aircraft*, Vol. 14, Feb. 1977, pp. 188-193.

[21]Fink, P.T. and Soh, W.K., "A New Approach to Roll-Up Calculations of Vortex Sheets," *Proceedings of the Royal Society of London, Series A*, Vol. 362, 1978, pp. 195-209.

[22]Baker, G.R., "A Test of the Method of Fink & Soh for Following Vortex-Sheet Motion," *Journal of Fluid Mechanics*, Vol. 100, Pt. 1, 1980, pp. 209-220.

[23]Hoeijmakers, H.W.M. and Vaatstra, W., "A Higher-Order Panel Method Applied to Vortex Sheet Roll-Up," *AIAA Journal*, Vol. 21, April 1983, pp. 516-523.

[24]Maltby, R.L., "Flow Visualization in Wind Tunnels Using Indicators," AGARDograph No. 70, 1962.

[25]Hummel, D. and Redeker, G., "Experimentelle Bestimmung der gebundenen Wirbellinien sowie des Strömungsverlaufs in der Umgebung de Hinterkante eines schlanken Deltaflügels," *Abhandlungen der Braunschweigschen Wissenschaftlichen Gesellschaft*, Vol. 22, 1972, pp. 273-290.

[26]Verhaagen, N.G., "Measurement of the Pressure Distribution on a Biconvex Delta Wing of Aspect Ratio 1," Dept. of Aeronautical Engineering, Delft University of Technology, Delft, the Netherlands, unpublished report, 1977.

[27]Verhaagen, N.G., "Experimental Investigation of the Vortex Flow Over Delta and Double-Delta Wings," Dept. of Aeronautical Engineering, Delft University of Technology, Delft, the Netherlands, Report LR-372, 1983.

[28]Earnshaw, P.B. and Lawford, J.A., "Low-Speed Wind-Tunnel Experiments on a Series of Sharp-Edged Delta Wings," Aeronautical Research Council, R&M No. 3424, 1966.

[29]Küchemann, D., *The Aerodynamic Design of Aircraft*, 1st ed., Pergamon Press, New York, 1978, p. 254.